Oral presentation | 4 JSAP-Optica Joint Symposia 2024：4.1 Plasmonics and Nanophotonics

Tue. Sep 17, 2024 9:00 AM - 12:00 PM JST | Tue. Sep 17, 2024 12:00 AM - 3:00 AM UTC A34 (TOKI MESSE 3F)

[17a-A34-1~9] 4.1 Plasmonics and Nanophotonics

Nicholas Smith(Osaka Univ.)

English Presentation
9:00 AM - 9:30 AM JST | 12:00 AM - 12:30 AM UTC
[17a-A34-1]
[JSAP-Optica Joint Symposia Invited Talk] Selective Accumulation of SERS Signal
○Yuika Saito[1], Takahiro Kondo[1], Kota Uchiyama[1] (1.Gakushuin Univ.)

English Presentation
9:30 AM - 10:00 AM JST | 12:30 AM - 1:00 AM UTC
[17a-A34-2]
[JSAP-Optica Joint Symposia Invited Talk] Contribution of sub-radiant plasmon resonance to surface-enhanced spectroscopy
○Tamitake Itoh[1], Yuko S. Yamamoto[2] (1.AIST, 2.JAIST)

English Presentation
10:00 AM - 10:15 AM JST | 1:00 AM - 1:15 AM UTC
[17a-A34-3]
Optical chirality enhancement at the nanoscale using inversely-designed 3D nanogap antennas
○Atsushi Taguchi[1], Keiji Sasaki[1] (1.Hokkaido Univ.)

Presentation by Applicant for JSAP Young Scientists Presentation Award English Presentation
10:15 AM - 10:30 AM JST | 1:15 AM - 1:30 AM UTC
[17a-A34-4]
Surface-enhanced Fluorescence by Mie Resonant Silicon Nanosphere Monolayer
○(M2)VU THI OANH[1], HIROSHI SUGIMOTO[1], MINORU FUJII[1] (1.Kobe Univ.)

Presentation by Applicant for JSAP Young Scientists Presentation Award English Presentation
10:45 AM - 11:00 AM JST | 1:45 AM - 2:00 AM UTC
[17a-A34-5]
SERS Detection of Chemical Reactions Induced by Optical Heat
○(D)Balaji Sanap[1], Takuo Tanaka[1,2], Taka-aki Yano[1,2] (1.Tokushima University, 2.RIKEN)

English Presentation
11:00 AM - 11:15 AM JST | 2:00 AM - 2:15 AM UTC
[17a-A34-6]
Bessel Beam-Instigated Two-Fold SERS Enhancement in AuNP Structures Compare to Drop Casting
○(D)Riya Choudhary[1], Kaushal Vairagi[2], Samir K. Mondal[2], Sachin K. Srivastava[1,3] (1.Dept. of Physics, IIT Roorkee, 2.micro-NOC, CSIR-CSIO, 3.CPQCT, IIT Roorkee)

English Presentation
11:15 AM - 11:30 AM JST | 2:15 AM - 2:30 AM UTC

[17a-A34-7]

【No-Show】High-Sensitivity Plasmonic Sensors Probe for Uric Acid Detection using Surface Funtionalized Gold-Graphene Quantum Dotes stacked Nanocomposites

○AHMAD SHUKRI MUHAMMAD NOOR[1,2], Olabisi Abdullahi Onifade[1,2], Muhammad Hafiz Abu Bakar[1,2], Mohd Adzir Mahdi[1,2] (1.Department of Computer and Communication Systems Engineering, Faculty of Engineering, Universiti Putra Malaysia, 2.Wireless and Photonics Research Centre of Excellence, Faculty of Engineering, Universiti Putra Malaysia)

English Presentation

11:30 AM - 11:45 AM JST | 2:30 AM - 2:45 AM UTC

[17a-A34-8]

Enhanced Red Emission in Europium-Doped Niobate Phosphors for High-Efficiency Warm White LEDs

○(DC)Kanishk Poria[1], Nisha Deopa[2], Jangvir Singh Shahi[1] (1.Panjab Univ., 2.Ch. Ranbir Singh Univ.)

English Presentation

11:45 AM - 12:00 PM JST | 2:45 AM - 3:00 AM UTC

[17a-A34-9]

Probing Forbidden Low-Frequency Raman Modes in MoS_2 via Plasmonic Nanoparticle

○(D)Zhen Zong[1], Ryosuke Morisaki[1], Kanami Sugiyama[2], Masahiro Higashi[3], Takayuki Umakoshi[1], Prabhat Verma[1] (1.Osaka Univ., 2.Kyoto Univ., 3.Nagoya Univ.)

表面増強ラマン散乱の選択的信号積算

Selective Accumulation of SERS Signal

学習院大理[1]　○齊藤 結花[1]，近藤 崇博[1]，内山 高汰[1]

Gakushuin Univ.[1], ○Yuika Saito[1], Takahiro Kondo[1], Kota Uchiyama[1]

E-mail: yuika.saito@gakushuin.ac.jp

We developed a new method for obtaining surface-enhanced Raman scattering (SERS) spectra with extremely high sensitivity and spectral resolution[1]. In this method, thousands of SERS spectra are acquired, followed by a data selection procedure based on density-based spatial clustering of applications with noise (DBSCAN)[2]. Each spectrum is recorded by exposure with a single nanosecond laser pulse to avoid the effect of time averaging. The reconstructed spectrum consists of the data which belong to the clusters. The method was applied to a crystal violet (CV) aqueous solution 10^{-7} mol/L.

Methods

The data selection using DBSCAN is firstly, thousands of SERS spectra were acquired, with each spectrum measured by a single-shot nanosecond laser pulse to avoid time averaging. Secondly, an intensity–wavelength plot (I–W plot) was constructed by extracting the data sets of the highest intensity and its pixel number from each SERS spectrum. Thirdly, we applied DBSCAN to the I–W plot to automatically separate the signal (cluster) from the noise (non cluster). DBSCAN process classify the high density of data points as a cluster, and the other part as a noise.

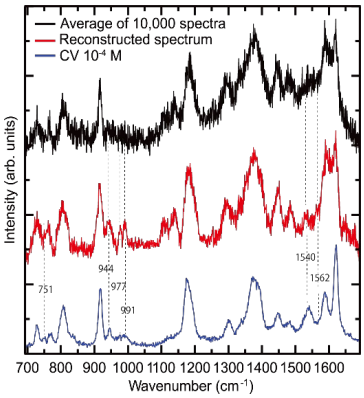

Figure 1. Reconstructed single-pulsed SERS spectra of 10^{-7} mol/L CV (532 nm excitation). Red line: DBSCAN reconstruction, Black line: Average of all (10,000) spectra, Blue line: thick solution.

Results

Figure 1 shows the Raman spectra of CV, reconstructed by single-pulsed SERS with DBSCAN. The red line indicates the reconstructed spectrum obtained by DBSCAN, while the black line indicates the average of 10,000 single-pulsed spectra. For comparison, a spectrum of high-concentration CV solution (10^{-4} mol/L) is shown by the blue line. According to Figure 1, it can be observed that the reconstructed spectrum improved signal-to-noise ratio in comparison with the averaged spectrum. The peaks 751, 944, 977, 991 cm^{-1} are clearly recognized in the red spectra, while in the black spectra, these peaks are difficult to see. Similarly, the peak at 1540 and 1562 cm^{-1} is more easily observed in the red spectrum than in the black spectra. These results suggest that we successfully recovered all the Raman peaks found in the spectrum under high concentration.

References

[1] Kondo T., Saito Y., *J. Phys. Chem. A* (2022); **126,** 1755-1760.
[2]Ester, M.; Kriegel, H.-P.; J. Sander; X. Xu., *KDD-96 proceedings* (1996) 226–231.

表面増強分光における準放射プラズモン共鳴の寄与

Contribution of sub-radiant plasmon resonance to surface-enhanced spectroscopy

産総研健医工 [1]，北陸先端大 [2]，○伊藤 民武 [1]，山本 裕子 [2]

AIST[1], JAIST[2], ○Tamitake Itoh[1], Yuko S. Yamamoto[2]

E-mail: tamitake-itou@aist.go.jp

The electromagnetic (EM) mechanisms of surface-enhanced spectroscopy e.g. surface-enhanced Raman scattering (SERS) and surface-enhanced fluorescence (SEF) have been examined using superradiant plasmon resonance, such as the dipole or dipole–dipole (DD) coupled plasmon resonance localized at the gaps between small and symmetric metallic nanoparticle (NP) dimers [1]. The large EM enhancement of DD-coupled resonance at the gaps, namely hotspots (HSs), has received considerable attention because HSs exhibit exotic phenomena such as cw laser excited nonlinear emissions, ultrafast SEF, vibrational pumping, and the field gradient effect [2]. Furthermore, the EM coupling energy between DD-coupled plasmons and a molecular excitons at the HSs exceeds several hundred millielectronvolts, resulting in new physics and chemistry e.g. strong coupling, molecular optomechanics, and polariton chemistry [2,3].

However, higher-order plasmon resonance, such as the dipole–quadrupole (DQ) coupled plasmon resonance, which is subradiant, mainly determines the EM enhancement for large or asymmetric NP systems. Thus, clarifying the contribution of the subradiant resonance to EM enhancement is important for evaluating various plasmonic systems for SERS related spectroscopies and phenomena [4-7].

First, the contribution of DQ coupled plasmon resonance to EM enhancement is explained using the spectral uncorrelation between the experimentally obtained SERS with ultrafast SEF and the Rayleigh scattering spectra of silver NP dimers [4]. Second, the radiation properties of the SERS light generated by the DQ coupled resonance were determined through EM calculations [5]. Third, the importance of absorption spectroscopy in the evaluation of DQ coupled resonance is clarified based on quantum optics [6]. Finally, we introduce a method to directly evaluate the EM enhancement factors induced by DQ coupled resonance using ultrafast SEF [7].

References

[1] T. Itoh, Y. S. Yamamoto, and Y. Ozaki, *Chem. Soc. Rev.* 2017, **46**, 3904-3921.

[2] T. Itoh, M. Prochazka, Z.-C. Dong, W. Ji, Y. S. Yamamoto, Y. Zhang, and Y. Ozaki, *Chem. Rev.* 2023, **123**, 1552-1634.

[3] T. Itoh, and Y. S. Yamamoto, *Nanoscale* 2021, **13**, 1566-1580.

[4] T. Itoh, and Y. S. Yamamoto, *J. Phys. Chem. C* 2023, **127**, 5886–5897.

[5] T. Itoh, and Y. S. Yamamoto, *J. Phys. Chem. B* 2023, **127**, 4666-4675.

[6] T. Itoh, and Y. S. Yamamoto, *J. Chem. Phys.* 2023, **159**, 2 034709.

[7] T. Itoh, and Y. S. Yamamoto, *J. Chem. Phys.* 2024, **160**, 024703.

Optical chirality enhancement at the nanoscale using inversely-designed 3D nanogap antennas

Hokkaido Univ.[1], ○Atsushi Taguchi[1], Keiji Sasaki[1]
E-mail: taguchi@es.hokudai.ac.jp

We present a 3D nanogap antenna with a high chiral dissymmetry—the field intensity at the nanogap is high for a particular handedness of circularly polarized incident light while not for the other[1]. The antenna structure was found using a computational inverse design technique called topology optimization. With circularly polarized incident light implemented into the algorithm, a spiral structure was created that is too complex to attain by human intuition or imagination. We calculated the near-field intensity at the nanogap of the structure, and the resultant dissymmetry factor was as high as 1.40. We also found a 50-fold enhancement of the optical chirality within the nanogap compared to that of the circularly polarized plane wave propagating in the free space. The chirality enhancement was elucidated with a fluid model of the chirality flux within the 3D nanoantenna, which is then correlated to light' s spin angular momentum (SAM). This finding can be a novel design strategy to enhance optical chirality density at the nanoscale using nanophotonic structures, potentially revolutionizing the field of nanophotonics and plasmonics.

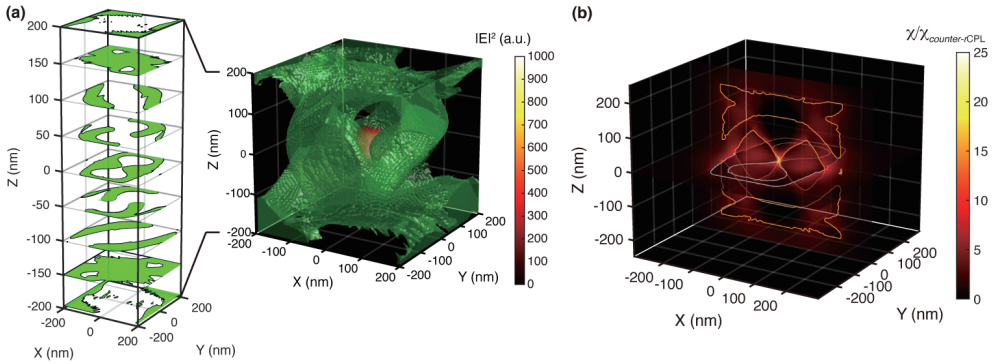

Figure 1: (a) A 3D-rendered model of the topology-designed structure (right) and Z-sliced sections at a 50-nm interval (left). The structures were optimized for a counter-propagating circularly polarized light traveling along the Z axis. The electric field intensity distribution is overlaid in the right panel. The material is TiO_2. (b) Optical chirality density, χ, normalized to that without the structure, displayed at planes $Z = 0$ nm and $Y = 0$ nm.

References

[1] A. Taguchi, *et al.*, arXiv:2402.10742 [physics.optics].

Surface-enhanced Fluorescence by Mie Resonant Silicon Nanosphere Monolayer

Kobe Univ [1], ◦(M2) Vu Thi Oanh[1], Hiroshi Sugimoto[1], Minoru Fujii[1]

E-mail: sugimoto@eedept.kobe-u.ac.jp

Surface-enhanced fluorescence (SEF) biosensors are vital for biomedical applications due to their exceptional sensitivity, enabling rapid and precise analyses. Compared to plasmonic resonators suffering from high Ohmic losses, dielectric Mie resonators exhibit lower losses and higher Q resonances. As a dielectric Mie resonator, silicon (Si) nanosphere (NS) with diameters of 100–250 nm is an almost ideal candidate for SEF biosensors due to their strong Mie resonances in the range of visible to near-infrared wavelengths. So far, Si nanostructure arrays have been fabricated with high precision by using electron-beam lithography on a solid substrate. However, it is challenging to create arrays larger than a millimeter scale for naked-eye readable biosensors.

In this work, the monolayers of Si NS with diameters of 100 to 250 nm [1] developed in our group are studied for a surface-enhanced fluorescence biosensor platform. Figure 1a shows the photographs of the monolayers fabricated by drop-casting colloidal Si NSs with different average diameters onto amino-modified SiO_2 substrates (1 cm × 1 cm). The filling factor is fixed to ~60% for all the samples. Figure 1b shows the corresponding reflectance spectra, demonstrating the size-tunable Mie resonance peaks at 430 to 800 nm. The fabricated Si NS monolayer substrates were functionalized with fluorophores (Lucifer Yellow) and the fluorescence properties were studied under an optical microscope (Fig. 2a). The averaged fluorescence spectrum obtained from 100 different spots of the monolayer with the average Si NS diameter of 128.7 nm (Fig. 2) shows about 14-fold enhancement with respect to that of the reference. In the presentation, from the comparison with the calculation results, we will discuss the size dependence of the fluorescence enhancement factor in detail.

[1] Tanaka, H et al. *ACS Appl Nano Mater* 7, 2605–2613 (2024).

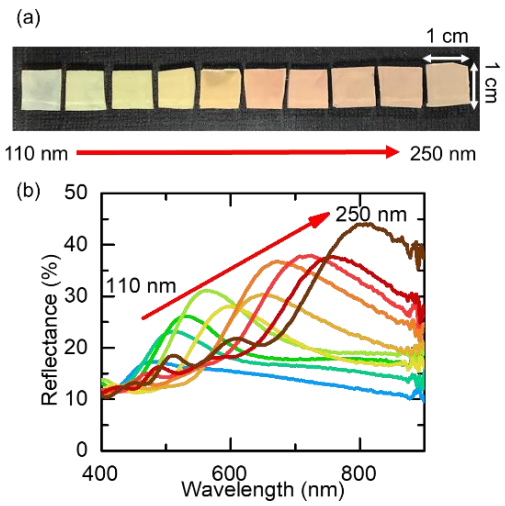

Fig. 1 (a) Photographs and (b) reflectance spectra of Si NS monolayer with different average diameters.

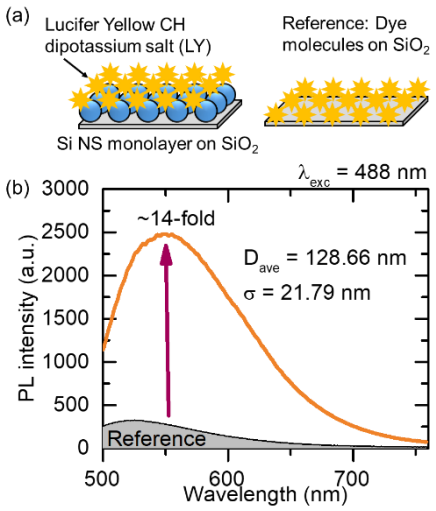

Fig. 2 (a) Illustration of dye molecules attached on the top of a Si NS monolayer and a SiO_2 substrate. (b) Photoluminescence spectra of dye molecules on a Si NS monolayer and a SiO_2.

SERS Detection of Chemical Reactions Induced by Optical Heat

Tokushima Univ. [1], RIKEN [2], ○Balaji Sanap[1], Takuo Tanaka[1,2], Taka-aki Yano[1,2]

E-mail: yano.takaaki@tokushima-u.ac.jp

Surface Enhanced Raman Scattering (SERS) is a powerful technique that enables molecular fingerprint-based ultra-sensitive detection through an enhanced electromagnetic field generated by plasmonic metal nanoparticles. This technique has found extensive use in various fields, including chemical sensing, biological imaging, and photochemical reactions, due to its ability to enhance reaction rates and decrease energy barriers at the nanoscale.

In this study, we demonstrated SERS detection of a chemical reaction induced by optical heat generated in the vicinity of plasmonic nanoparticles and substrates. As schematically shown in Fig. 1(a), the generated heat facilitates an interaction between the amine group (-NH_2) of 4-aminothiophenol adsorbed on the smooth Ag metallic surface and the carboxylic acid (-COOH) of 4-mercaptobenzoic acid adsorbed on the Au nanoparticle. This interaction leads to the formation of an amide bond through dehydration, identified by the new appearance of specific vibrational peaks. Notably, a newly appeared vibrational mode at 521 cm^{-1}, indicated by the arrow in the SERS spectrum (Fig. 1(b)), was observed. According to quantum chemical simulation based on density functional theory, this peak is attributed to the bending between the nitrogen and hydrogen of the amide group. The simulations also indicate that the vibration of the C=O bond shifted to a lower wavenumber region due to the formation of the amide bond.

These findings highlight the potential of using SERS to monitor chemical reactions at the molecular level, providing insights into reaction mechanisms facilitated by plasmonic nanostructures. Further research may explore the applications of this technique in other types of chemical reactions and its integration with other analytical methods.

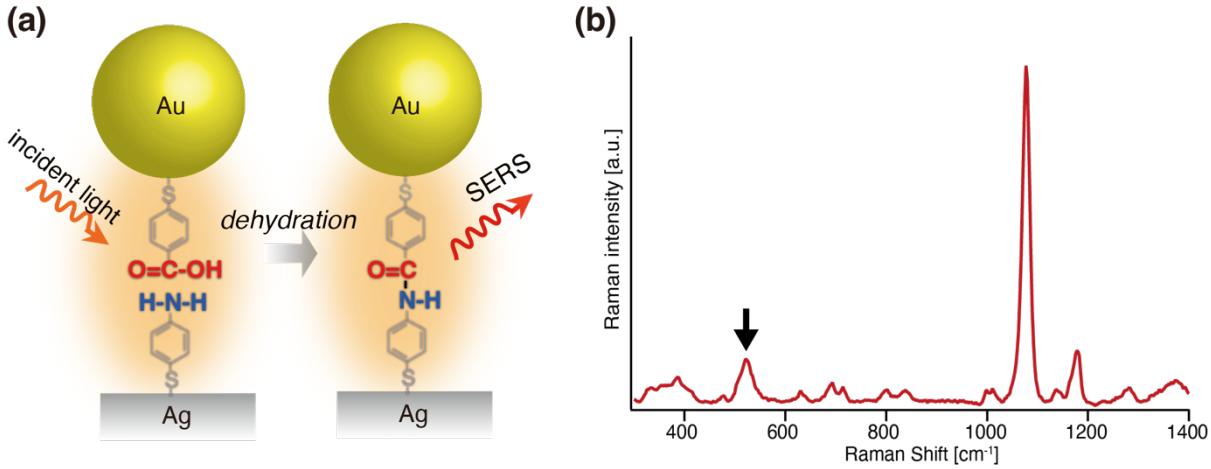

Figure 1: (a) Schematic of chemical reaction (amide bond formation) through optical heat generated between a plasmonic nanoparticle and substrate, (b) the corresponding SERS spectrum.

Bessel Beam-Instigated Two-Fold SERS Enhancement in AuNP Structures Compare to Drop Casting

Riya Choudhary[1], Kaushal Vairagi[2], Samir K. Mondal[2], Sachin K. Srivastava[1,3]

[1] Department of Physics, Indian Institute of Technology Roorkee, Roorkee- 247667, India
[2] μ-NOC, CSIR-CSIO, Chandigarh-160030, India
[3] CPQCT, Indian Institute of Technology Roorkee, India
E-mail: sachin.srivastava@ph.iitr.ac.in

1. Introduction

Since the discovery of SERS, due to its high sensitivity, it has been widely used in various fields such as biosensing, chemical sensing, and food safety etc., [1]. In SERS, when a probe molecule is placed near a metallic nanostructure it feels a localized field generated due to localized surface plasmons (LSPs) which effectively amplifies its Raman signal. The LSPs are the collective oscillation of free electrons in metallic nanostructures [2]. For the fabrication of the SERS active substrates various methods have been introduced to arrange the metallic nanoparticles (NPs) in specific morphologies and arrangements [3]. Optical forces of a laser beam can be employed to arrange metallic NPs efficiently on a substrate [4].

2. Results and discussions

In Fig.1(a-d), scanning electron microscope (SEM) image of the axicon tip, microscopic image of Bessel beam, SEM images of gold (Au) NPs dried with Bessel beam and without illumination of light are shown respectively. AuNPs dried with Bessel beam illumination are arranged in the Bessel beam rings, while AuNPs were drop cast and dried without illumination of light are agglomerated as can be seen from SEM images in Fig.1 (d). The Raman spectra has been recorded with a fiber optic Raman probe coupled to laser of excitation wavelength 785 nm. The recorded Raman spectra of R6G on coverslip is shown in Fig.2 (a) in absence of AuNPs, in presence of AuNPs with Bessel beam illumination and without illumination of light. It can be seen clearly from the figure that in presence of AuNPs, Raman signal enhances even if there is no illumination of light but the enhancement in Raman signal increases when we illuminate with Bessel beam. In Fig.2 (b), the Raman spectra recorded for 4-ATP molecule on reflecting substrate (Si/Ag substrate) is shown for Bessel beam illumination, without illumination of light and without AuNPs. It can be seen from the figure that there is more enhancement in Raman signal of 4-ATP molecule in case of Bessel beam illumination on reflecting substrate similar to transmitting substrate.

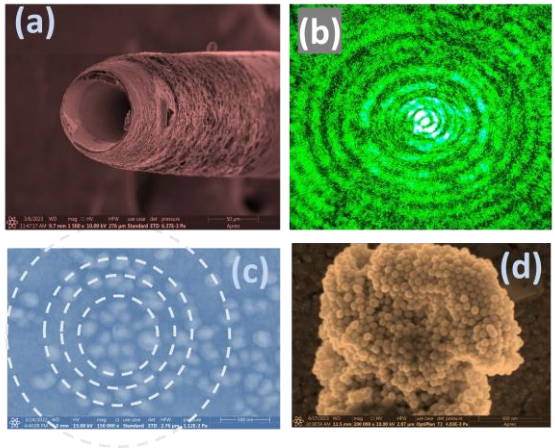

Fig.1. (a) SEM image of axicon tip, (b) microscopic image of Bessel beam, SEM image of AuNPs dried (c) with Bessel beam illumination, and (d) without illumination of light.

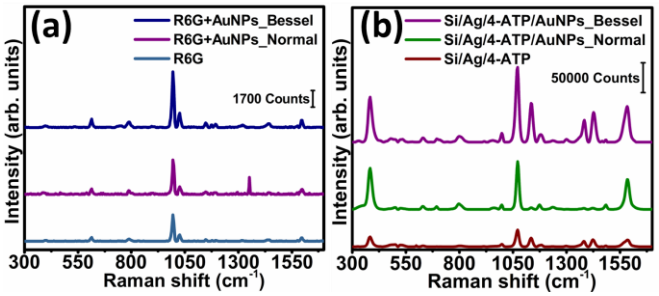

Fig.2. SERS spectra of (a) R6G in transmission mode (b) 4-ATP in reflection mode.

3. Conclusions

We have shown 2-fold enhancement in SERS signal of R6G and 4-ATP molecules on transmitting and reflecting substrates respectively with Bessel beam illumination as compared to without illumination of light (drop casting method).

Acknowledgements

We would like to express sincere thanks to MoE-STARS, DST-BDTD, and IIT Roorkee. Riya Choudhary thanks to Council of Scientific & Industrial Research (CSIR) -India for fellowship.

References

[1] J. Langer et al., ACS Nano **14** (2020) 28.
[2] M. Pelton, and G. Bryant, Hoboken, NJ, John Wiley & Sons, 2013.
[3] J. Dong et al., Opt. Express **31** (2023) 21225.
[4] R. Choudhary et al., J. Appl. Phys. **135** (2024) 073104.

High-Sensitivity Plasmonic Sensors Probe for Uric Acid Detection using Surface Funtionalized Gold-Graphene Quantum Dotes stacked Nanocomposites

Department of Computer and Communication Systems Engineering, Faculty of Engineering, Universiti Putra Malaysia, Wireless and Photonics Network Research Centre of Excellence, Faculty of Engineering, Universiti Putra Malaysia[2]

[o]Ahmad Shukri Muhammad Noor[1,2], Olabisi Abdullahi Onifade[1,2], Muhammad Hafiz Abu Bakar[1,2], Mohd Adzir Mahdi[1,2]
E-mail: ashukri@upm.edu.my

This study introduces a surface-functionalized sensor probe incorporating 3-aminopropyltriethoxysilane (APTES) self-assembled monolayers (SAM) on a Kretschmann-configured plasmonic sensor. The probe employs stacked nanocomposites of gold deposited through sputtering and graphene quantum dots (GQD) deposited via spinning, enabling highly sensitive and accurate uric acid (UA) detection within the physiologically relevant concentration range. Comprehensive characterization of the sensor probe was conducted and validated through field emission scanning electron microscopy (FESEM), energy-dispersive X-ray spectroscopy (EDX), and Fourier transform infrared spectroscopy (FTIR) techniques. Surface functionalization yielded a 60.64% increase in sensitivity for the sensor probe, resulting in values of 0.0221°/(mg/dL) for gold–GQD probe and 0.0355°/(mg/dL) for gold–APTES–GQD probe, accompanied by linear correlation coefficients of 0.8249 and 0.8509, respectively. The highest sensitivity achieved was 0.0706°/(mg/dL), exhibiting a linear correlation coefficient of 0.993 and a low limit of detection (LOD) of 0.2 mg/dL. Furthermore, surface functionalization significantly enhanced binding affinity, as evidenced by Langmuir constants of 14.29 μM^{-1} for the gold–GQD probe and 0.0001 μM^{-1} for the gold–APTES–GQD, probe representing a remarkable 142,900-fold increase. The functionalized sensor probe demonstrated notable reproducibility and repeatability, with relative standard deviations of 0.166% and 0.013%, respectively, along with exceptional temporal stability of 99.66%. These findings represent a transformative leap in plasmonic UA sensors, delivering a marked enhancement in precision, reliability and substantial increase in sensitivity.

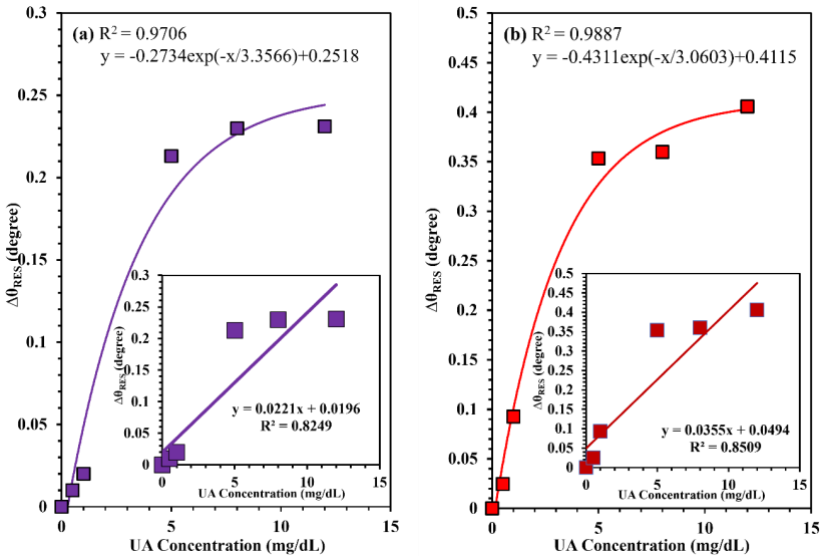

Figure 1: Fitting curves and linearity plots for (a) gold–GQD sensor probe at 60 nm configuration exhibits a sensitivity of 0.0221°/(mg/dL)and (b) gold–APTES–GQD sensor probe at 60 nm configuration boasts a higher sensitivity of 0.0355°/(mg/dL)

References

1. O.A. Onifade, Z.-H.M. Zin, M.H.B.A. Bakar, M.T. Alresheedi, M.A. Bin Mahdi, A.S.M. Noor, Salivary Uric Acid Detection With Graphene-Gold Bilayers Surface Plasmon Resonance, IEEE Sens J. (2023) 1–1. https://doi.org/10.1109/JSEN.2023.3319702.
2. D. Dey, T. Goswami, Optical biosensors: A revolution towards quantum nanoscale electronics device fabrication, J Biomed Biotechnol. 2011 (2011). https://doi.org/10.1155/2011/348218.

Enhanced Red Emission in Europium-Doped Niobate Phosphors for High-Efficiency Warm White LEDs

Kanishk Poria[1], **Nisha Deopa**[2], **Jangvir Singh Shahi**[1]

[1]*Department of Physics, Panjab University, Chandigarh-160014, India*
[2]*Department of Physics, Chaudhary Ranbir University, Jind-126102, India*
E-mail: kanishk.chaudhary15@gmail.com

1. Introduction

Rare-earth doped crystalline materials are of significant interest for photonic and optoelectronic applications, particularly in phosphor-converted white-light-emitting diodes (pc-WLEDs), which offer high brightness, energy efficiency, compact size, durability, and environmental friendliness. However, pc-WLEDs lack a red color component. To address this, europium-doped niobate-based phosphors were synthesized using a high-temperature solid-state reaction technique at 1300°C[1].

2 Results and Discussions

The XRD patterns of both undoped and Eu-doped phosphors showed excellent crystallinity and phase purity, with diffraction peaks matching the standard JCPDS data, indicating that Eu^{3+} ions did not alter the tetragonal tungsten bronze (TTB) structure. Photoluminescence excitation (PLE) spectra for Eu^{3+}-doped niobate phosphors across various concentrations (1.0-10.0 mol%) revealed efficient excitation at 392 nm (near-UV) and 466 nm (blue). Photoluminescence (PL) spectra under 392 nm excitation displayed five main emission peaks (550-700 nm), with the optimal Eu^{3+} concentration at 9.0 mol% to avoid quenching. The internal quantum yield (IQE) measures the efficiency of converting electrical power into optical power for a phosphor, with IQE representing the ratio of emitted to absorbed photons and external quantum efficiency (EQE) representing the ratio of emitted to incident photons. For optimal Eu^{3+}-doped phosphor, IQE, absorption efficiency, and EQE under 392 nm excitation are more than 90%, 60%, and 55%, respectively. These high values, along with color coordinates close to standard red phosphors, indicate their potential for use in warm white LEDs.

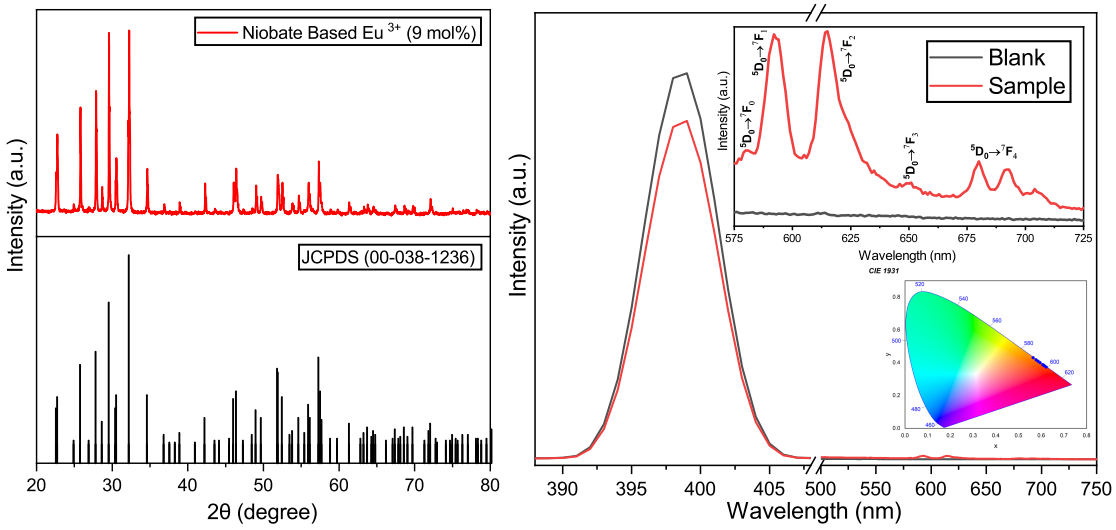

Figure 1: (a) XRD pattern for JCPDS and optimal phosphor. (b) Enhanced internal quantum yield for optimal phosphor (Inset: CIE cromaticity diagram)

[1] Poria K, Lohan R, Bhatia S, Kumar A, Singh R, Deopa N, Punia R, Shahi JS, Rao AS., "Lumino-structural properties of Dy3+ activated Na3Ba2LaNb10O30 phosphors with enhanced internal quantum yield for w-LEDs", RSC adv. **13** 11557-68 (2023).

Probing Forbidden Low-Frequency Raman Modes in MoS_2 via Plasmonic Nanoparticle

Zhen Zong[1], Ryosuke Morisaki[1], Kanami Sugiyama[2], Masahiro Higashi[3], Takayuki Umakoshi[1,4], Prabhat Verma[1]
[1] Dept. of Applied Physics, Osaka Univ., [2] Dept. of Molecular Engineering, Kyoto Univ., [3] Dept. of Complex Systems Science, Nagoya Univ.,[4] Institute of Advanced Co-Creation Studies, Osaka Univ.
E-mail : verma@ap.eng.osaka-u.ac.jp

1. Introduction

Interlayer interaction through the van der Waals forces in two-dimensional (2D) materials like molybdenum disulfide (MoS_2) determine most of the layer properties, which shows up as low-frequency modes (less than 50cm^{-1}) in Raman scattering. But the weak low-frequency signals are often obscured by background noise, requiring enhancement techniques [1]. Furthermore, detecting forbidden low-frequency Raman modes poses additional challenges. These modes, suppressed by symmetry selection rules, provide important information into molecular structures and electronic properties but are not observed in conventional Raman spectroscopy as they are symmetry forbidden. Our approach can detect forbidden low-frequency modes and achieve high-sensitivity through low-frequency surface-enhanced Raman spectroscopy (LF-SERS).

2. Result and discussion

We utilize silver nanoparticles to detect forbidden low-frequency Raman modes in MoS_2 by breaking the selection rules. The strong gradient of near-field light with sharply varying intensity within a nanometric volume near the nanoparticle causes selective symmetry breaking as shown in Fig.1. This breaks the Raman selection rules, allowing the observation of vibration patterns that are forbidden in Raman spectroscopy [2].

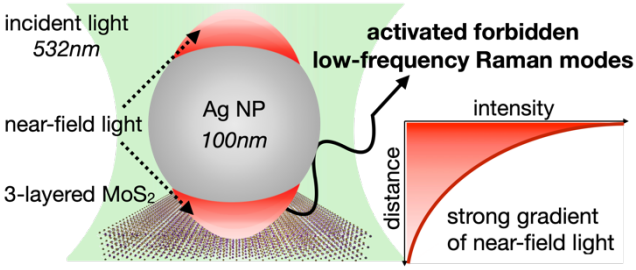

Figure 1. Gradient near-field light in the vicinity of a nanoparticle.

We used 3-layered MoS_2 as the sample and placed silver nanoparticles on its surface. We measured a LF-SERS image constructed with its breathing and shear modes at 28 cm^{-1} and observed high-intensity Raman signals only around the nanoparticle, as shown by the bright areas in Fig. 2(a). MoS_2 has four vibration modes in the low-frequency range: the breathing and the shear modes, both appearing at 28 cm^{-1}, are Raman-active, while the E" (15 cm^{-1}) and A_2" (46 cm^{-1}) modes are forbidden in Raman scattering. The forbidden Raman modes can only be activated near an isolated single particle as seen in Fig. 2(b). An AFM image and a SERS image from one of the isolated single particles are shown in Figs. 2(c) and 2(d), respectively. We demonstrate how LF-SERS changes with the gradient near-field light around this nanoparticle, which are measured from the points marked in Fig. 2(d). The forbidden Raman modes only appear in region with a strong gradient, as shown in the spectrum by the blue areas in Fig.2(e).

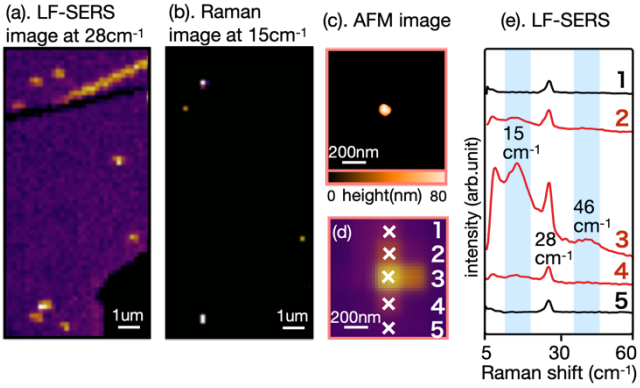

Figure 2. Forbidden LF-SERS image and spectrum.

To confirm our experimental results, we used calculations based on the density functional theory (DFT) to simulate Raman spectrum of a 3-layered MoS_2. Our simulations confirm the existence of forbidden Raman modes in MoS_2, with the vibration modes calculated by DFT matching the two forbidden Raman peaks detected in our experiments. Without the silver nanoparticles, these vibration modes are present but have zero intensity, indicating they are Raman-forbidden. The DFT calculations further reveal that the activation of these modes is not only due to the strong gradient near-field light but also involves physical contact deformation and charge transfer between the MoS_2 and the silver nanoparticles.

3. Conclusions

Our technique enables the first observation of LF-SERS and plasmonically activated forbidden low-frequency Raman modes in MoS_2, providing more information into the material's vibrational properties and advancing material characterization methods.

References

[1] P. Verma et al., Sci Rep 10, 21227 (2020).
[2] K. Ikeda et al., J. Am. Chem. Soc. 135 (2013).